# Modelling of auxin transport affected by gravity and differential radial growth

Loïc Forest[a,*,1], Fernando Padilla[b,1], Salomé Martínez[b,c], Jacques Demongeot[a,d], Jaime San Martín[b,c]

[a]*Laboratoire Techniques de l'Imagerie, de la Modélisation et de la Cognition (TIMC UMR CNRS 5525), Institut d'Ingénierie de l'Information de Santé, Pavillon Taillefer, Faculté de Médecine, 38706 La Tronche cedex, France*

[b]*Centro de Modelamiento Matemático (CMM UMR CNRS 2071), Av. Blanco Encalada 2120 piso 7, Santiago de Chile, Chile*

[c]*Departamento de Ingenería Matemática, Universidad de Chile, Av. Blanco Encalada 2120 piso 5, Santiago de Chile, Chile*

[d]*Institut Universitaire de France*

**Abstract**

When a tree stem deviates from verticality, as a result of different environmental factors, patterns of differential radial growth appear. Higher rates of wood production have been observed on the lower side of the tree and lower rates in the opposite side. Biological studies on plant hormones have shown that the concentration of auxin induces radial growth. They also have demonstrated the redistribution of auxin transport in response to gravity. Auxin is then designated as a mediator for differential growth.

This paper presents a model for three-dimensional (3-D) auxin transport in conifer trees, which includes gravity dependence. We obtain realistic heterogeneous patterns of auxin distribution over the tree. Then, we propose a law of growth based on auxin concentration to simulate successive differential radial growths. The predicted growths are compared with experimental results of reconstruction of 3-D annual growth of Radiata pine.

*Keywords:* Auxin transport; Radial growth; Gravitropism; Differential growth; Deviated stem

## 1. Introduction

In woody plants, the radial growth of the stem occurs by the successive additions of layers of cells, which differentiate from the vascular cambium. Cambium is a continuous layer of cells called initials, located between the xylem and phloem, throughout the entire tree. Initials differentiate into xylem cells inward and into phloem cells outward of the cambium. As a result of this process, diameter of stems and roots increases (for a review see, Han, 2001; Harris, 1991; Larson, 1994). Often, plants change their pattern of growth rate in response to environmental stimuli such as light or gravity or in response to internal signals (Parker and Briggs, 1990). There exists much evidence about the influence of plant hormones on the regulation of cell division and cell expansion (Clare et al., 2000). As Davies (1995) indicates, the plant hormones influence physiological processes at low concentrations, mainly growth, differentiation and development.

The auxin indole-3-acetic acid (IAA) has long been recognized as an important hormone regulating a wide array of responses in the growth and development of plants (Goldsmith, 1977, 1993; Little and Savidge, 1987). For many years, studies on IAA have been carried out to determine whether or not plants redistribute or regulate the concentration of IAA to produce growth changes. However, the contradictory results from these experiments have not provided a complete understanding of how IAA regulates growth and the development of the vascular system. As Uggla et al. (1996) indicate, failure to develop a unifying concept for the role of IAA in the regulation of

*Corresponding author.

*E-mail address:* loic.forest@imag.fr (L. Forest).

[1]First authors.

patterns of vascular tissue in both, primary and secondary plant bodies, is due to a limited knowledge not only of IAA perception mechanism, but also of its metabolism, transport and final distribution.

Today, there are some universally accepted propositions about auxins, such as buds and developing leaves are the major sources of IAA (Aloni, 2004; Goldsmith, 1977; Little and Savidge, 1987; Parker and Briggs, 1990), or that IAA is transported in a basipetal polar fashion (Goldsmith, 1977; Lomax et al., 1995; Rashotte et al., 2003). Kaldeway (1984), cited by Uggla et al. (1998), indicates that apically produced IAA is actively transported in a basipetal polar transport system which has been localized in the cambial zone,[2] its differentiating derivatives and the phloem region. Uggla et al. (1996) found high concentration of IAA in the cambial zone and its immediate derivatives, which suggests that this region is either a site of biosynthesis, a site of IAA transport, or both. The velocity of transport of the IAA is 5–20 mm per hour in the shoots and coleoptiles of a wide range of plant species (Lomax et al., 1995).

Auxin has been involved as the major signal mediating tropic stimuli. In late 1920s, the Cholodny–Went hypothesis was formulated to explain the gravitropic response of plant roots and shoots. This hypothesis proposes that the differential growth rates during the gravitropic response are based on auxin redistribution and altered auxin transport within plant tissue (Evans, 1991). Strong support for this hypothesis comes from the ability of auxin transport inhibitors to completely abolish the gravity response in both roots and shoots (Katekar and Geissler, 1977; Muday and Haworth, 1994 cited by Lomax et al., 1995). Evidence of a redistribution of IAA due to gravitropism comes from many experimental works (Dolk, 1936; Friml et al., 2002; Funada et al., 1990; Gillespie and Thimann, 1963; Goldsmith and Wilkins, 1964; Ottenschläger et al., 2003; Parker and Briggs, 1990; Rashotte et al., 2000). Concerning the transport of auxin, the chemiosmotic model postulates that polar auxin transport occurs through the action of cellular auxin influx and efflux carriers located in the plasma membrane of transporting cells (Rubery and Sheldrake, 1974). This model proposes that the efflux carrier is asymmetrically localized at the basal side of cells determining the polarity of IAA transport in plant tissues. Several experimental works have been carried out to identify the protein involved in the transport of auxin. Friml et al. (2002) showed that asymmetric growth in *Arabidopsis* is correlated with an asymmetric auxin distribution. This follows redistribution of a protein, PIN3, laterally in the cell membrane. PIN3 is a likely candidate for an efflux component of the lateral auxin transport system. Bennett et al. (1996) reported a protein called AUX1, which could act as an auxin influx protein. Summarising, Muday et al. (2000) pointed out that two protein complexes control the auxin movement into and out of the cells, the auxin uptake carrier (AUX) and the auxin efflux carrier (PIN), which control the amount and direction of polar auxin transport.

Goldsmith (1977) points out that the evidence of a passive diffusion of IAA is provided by the fact that respiration inhibitors do not completely stop the uptake and efflux of auxin from individual cells. The specificity and saturability of the process also confirm mediation by protein components. This specific active protein-mediated transport is a critical component of a transport system that can be differentially regulated during plant growth, development, and response to the environment (Lomax et al., 1995). Moreover, these authors support the view that auxin transport is important in transduction of the gravity signal, not in its perception.

The results of Uggla et al. (1996) suggest that an increased basipetal supply of IAA to the vascular cambium during resumption of shoot growth results in a wider radial IAA distribution rather than a higher IAA concentration in the cell division zone. This observation provides further support for the concept that IAA controls cambial growth by determining the radial extent of dividing cells in the cambial zone through positional signalling. Furthermore, this concept would explain the relationship between IAA amount and the cambial growth found by these authors (Sundberg et al., 1991). Although there exist some evidences of the influence of other hormones on the growth processes, such as ethylene (Chen et al., 1999; Eklund and Little, 1998; Eklund and Tiltu, 1999), cytokinins (Chen et al., 1999) and gibberellins (Kalev and Aloni, 1998; Wang et al., 1997), IAA is considered to be an important growth regulator in plants.

Many experimental studies have been carried out to describe the role of auxin in formation of reaction wood (Du et al., 2004; Funada et al., 1990; Phelps et al., 1977; Sundberg et al., 1994; Yamaguchi et al., 1980; Wardrop and Davies, 1964), involving a redistribution of auxin or auxin-transport inhibitors. These findings suggest that the formation of reaction wood is associated with a high level of auxin to induce compression wood (gymnosperms) and low level of auxin for tension wood (angiosperms). However, other authors (Hellgren, 2003, Hellgren et al., 2004) point out that induction of reaction wood is not mediated by the IAA level in the cambial tissues, but by other factors such as auxin perception mechanisms or additional signals. Despite that the formation of compression wood is not completely understood, it is generally accepted that reaction wood is formed in xylem tissue in response to a non-vertical orientation of the stem (Plomion et al., 2000) and it is related with the intrinsic growth direction and hormonal influence (Sundberg et al., 1994). The reaction wood constitutes an important defect in wood quality, affecting the mechanical, physical and chemical properties of the wood, resulting in important losses in the conversion processes.

We have developed a model to explain a theoretical redistribution of IAA in the vascular cambium, as a result

[2]Cambial zone includes the vascular cambium and the adjacent layers of daughter cells in differentiating process.

of the natural diffusion and transport processes influenced by gravity. The model does not attempt to explain the complex transport system of IAA, which has not been completely elucidated, but it represents a simplified mechanism by which IAA is transported inside the tree and how gravity influences this process. We also present a simplified model of radial growth based on the predicted auxin distributions. Three-dimensional (3-D) patterns of growth are then compared with experimental ones.

## 2. Modelling of auxin transport

Mathematical models for auxin transport at least go back to the MGGM model due to Mitchison (1980) and Goldsmith et al. (1981). This is a 1-D model in which the transport of auxin occurs in a column of cells.

Kramer (2001) defines the *cambial surface* to represent the cambium as a surface, because cambium thickness is negligible compared to tree dimensions. Using this concept, he formulated a more recent model (2002), that considers auxin transport in a local vertical plane of the *cambial surface*.

In both models, the flux $\vec{J}$ of auxin concentration $C$ consists of two terms: one related to passive diffusion and one to active transport, i.e.

$$\vec{J} = D\nabla C + vC\vec{u}, \tag{1}$$

where $D$ is a matrix accounting for the anisotropy of the diffusion and $v$ is the velocity of the active transport along the direction defined by the unitary vector $\vec{u}$. In Kramer (2002), the direction of active transport is determined according to the orientation of the cambial cells. The change in auxin concentration is given by the following equation of mass conservation:

$$\frac{\partial C}{\partial t} = -\nabla \cdot \vec{J}. \tag{2}$$

In the model proposed by Kramer, the anisotropy of the diffusion is due to the fact that cellular membranes are the main barriers to diffusion and the vertically elongated shape of cambial cells facilitate the diffusion along the main axis of the cells. More precisely, Eq. (2) of mass conservation can be written as

$$\frac{\partial C}{\partial t} = -\nabla \cdot ((vC - D_{||}(\nabla C \cdot \vec{u}))\vec{u} - D_{\perp}(\nabla C \cdot \vec{w})\vec{w}), \tag{3}$$

where $D_{||} > D_{\perp}$ are the constants for longitudinal and transversal diffusion, respectively, and $\vec{w}$ is the unitary vector directly perpendicular to $\vec{u}$, which defines the transverse direction.

To be precise, we should remark that $\vec{J}$ and $C$ represent the average value of their 3-D analogues over cambial thickness. In this way, Eq. (3) is the conservation of mass law for averages over the cambial surface.

The auxin flux depends greatly on the vector field $\vec{u}$, which is called the *grain pattern*. Kramer used a second equation for the variations in the orientation of cambial cells. In a local vertical plane defined by coordinates $(\vec{x}, \vec{y})$, $\vec{u}$ can be defined by its angle $\phi$ with the direction $\vec{x}$: $\vec{u} = \cos(\phi)\vec{x} + \sin(\phi)\vec{y}$. The equation for the evolution of $\phi$ is

$$\frac{\partial \phi}{\partial t} = -\mu \nabla C \cdot \vec{w} + K\Delta\phi. \tag{4}$$

This equation shows that two effects are considered. The first term reflects that cambial cells tend to orient parallel to the flux of auxin with $\mu$ a positive proportionality constant. The second term is introduced as a smoothing effect. It can be interpreted as the tendency of cambial cells to orient parallel with respect to each other.

These equations were used to study the grain pattern generated in a local plane and not to investigate the distribution of auxin. This formulation cannot be directly used to model the gravitropism effect as a pure 3-D phenomenon. To our knowledge, the only mathematical model including the gravitropism effect is developed by Forest and Demongeot (in press) which uses a generalization of Eq. (3) to account for diffusion over cambial thickness. This model was defined in the cambium which is represented as a thin 3-D Cartesian domain. It stipulates that directions of auxin flow are the same as those of a theoretical laminar fluid submitted to gravity. So, it does not reflect the interaction between cambial cells reorientation and auxin transport. Moreover, as cambial thickness is very small compared to the other dimensions involved, the simulations of this model are limited by computational capacity.

One of the aims of this paper is to propose a more general model, which takes into account the effect of gravity on auxin transport over a 3D *cambial surface*, which we denote $S$. We propose that gravity strength influences auxin transport in the cambial cells. The changes from the vertical direction of a tree produce a redistribution of auxin, increasing the lateral movement of auxin relative to its longitudinal transport. As a consequence of auxin redistribution, it is produced a reorientation of growing cambial derivatives over time and the tree tends to verticality.

The 3-D system is now written with a new term in the equation for angle evolution. This term generally can be written as a function $f$, which depends on grain pattern angle and gravity. It states that cambial cells also tend to orient with respect to gravity as well as to auxin flux. Then, the new system in Cartesian coordinates is given by

$$\begin{cases} \frac{\partial C}{\partial t} = -\nabla \cdot ((vC - D_{||}(\nabla C \cdot \vec{u}))\vec{u} - D_{\perp}(\nabla C \cdot \vec{w})\vec{w}), \\ \frac{\partial \phi}{\partial t} = K\Delta\phi - \mu \nabla C \cdot \vec{w} + f(\phi, \vec{g}), \end{cases}$$

$$\text{in } S, t > 0. \tag{5}$$

We refer the reader to the Appendix for the deduction of the mass-transport equation.

Note that Eqs. (5) do not include a production or consumption term, mainly because the metabolism of auxin is poorly understood. Also, we should point out that the differential operators in Eqs. (5) are superficial.

The most simple equation that we can choose for $f$ is

$$f(\phi,\vec{g}) = \alpha\left(\vec{w}\cdot\frac{\vec{g}}{||\vec{g}||}\right), \tag{6}$$

where $\alpha$ is a positive proportionality constant for gravity effect.

The boundary conditions for this problem are going to be expressed using the notation of Fig. 1. On the top frontier $S_T$, which is taken orthogonal to $\vec{g}$, the auxin flux is vertical and constant. That is, on $S_T$

$$\phi_{|S_T} = -\frac{\pi}{2} \text{ and } \vec{J}_{|S_T} = -J_0\vec{z},$$

where $\vec{z}$ is the vector (0,0,1) in Cartesian coordinates, and $\vec{g} = -g\vec{z}$.

On the bottom frontier $S_B$ the flux and the grain pattern are free.

The geometry considered for system (5) is the cambial surface $S$. $S$ is a smooth surface parameterized by a function $\vec{r}(s,\theta)$ such that $\partial\vec{r}/\partial s\cdot\partial\vec{r}/\partial\theta = 0$ and $\vec{r}(s,\bullet)$ periodic. We define two tangent vectors to the surface $S$:

$$\vec{t}_1 = \frac{\partial\vec{r}}{\partial\theta}\left\|\frac{\partial\vec{r}}{\partial\theta}\right\|^{-1}, \quad \vec{t}_2 = \frac{\partial\vec{r}}{\partial s}\left\|\frac{\partial\vec{r}}{\partial s}\right\|^{-1}$$

and one normal vector

$$\vec{n} = \vec{t}_1\wedge\vec{t}_2,$$

defining a local orthonormal basis $(\vec{t}_1,\vec{t}_2,\vec{n})$. The vector $\vec{u}$ of cambial cells orientation is now defined by $\vec{u} = \cos(\phi)\vec{t}_1 + \sin(\phi)\vec{t}_2$ in the local basis. The transversal direction $\vec{w}$ is defined so as $\vec{u}\wedge\vec{w} = \vec{n}$ and $(\vec{u},\vec{w},\vec{n})$ is an other local orthonormal basis, adapted to the grain pattern.

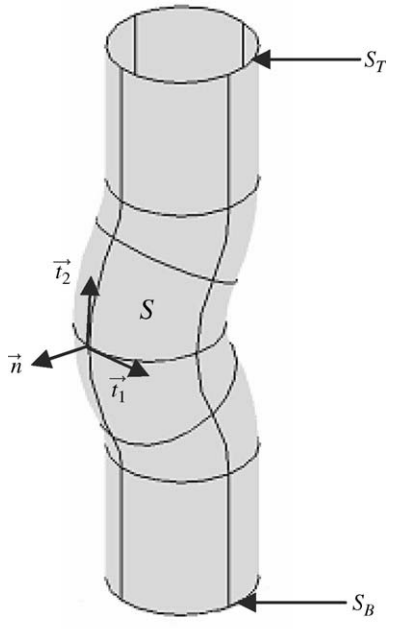


Fig. 1. Example of cambial surface geometry.

## 3. Results of auxin distribution in simple geometries

The solutions of PDE system defined above were determined using finite-element method. We used the software FEMLAB® 3.0 used in interaction with MATLAB® 6.5, which permits to solve PDE on surfaces. For our applications we consider the parameterization $\vec{r}:[0,L]\times[0,2\pi]\to\mathbb{R}^3$, of the form:

$$\vec{r}(s,\theta) = \vec{p}(s) + R\cos(\theta+\theta(s))\vec{n}_p(s) + R\sin(\theta+\theta(s))\vec{b}_p(s), \tag{7}$$

where $R$ is the radius of the tree taken constant. $\vec{p}:[0,L]\to\mathbb{R}^3$ represents the pith of the tree, parameterized using arc length. $\vec{n}_p$ and $\vec{b}_p$ are the normal and binormal vectors associated to $\vec{p}$, and $\theta'(s) = -\tau(s)$, $\tau(s)$ being the torsion of $\vec{p}$. According to this parameterization, $\vec{t}_2$ is chosen parallel to the pith and normal cross-sections to the surface are circles. $\vec{p}$ and $R$ are chosen so as $\vec{r}$ defines a smooth surface, using the condition $R\kappa(s)<1$, where $\kappa(s)$ is the curvature (as a reference see Do Carmo, 1976).

We used real order of magnitude for physical parameters of Eq. (5). For all the simulations, unless it is precised to other values, these parameters values are the following: $J_0 = 50\,\text{ng/cm/h}$, $v = 1\,\text{cm/h}$, $D_\parallel = 0.05\,\text{cm}^2/\text{h}$, $D_\perp = D_\parallel/5$, $g = 9.81\,\text{m/s}^2$. Value of velocity is taken from (Goldsmith et al., 1981), those of diffusion and flux from Kramer (2001). Reference parameters values for the angle equation are $K = 100\,\text{cm}^2/\text{h}$, $\mu = 2\,\text{cm}^3\,\text{rad/ng/h}$ and $\alpha = 5\,\text{rad/h}$. We use $f$ as defined by (6) and we also assume that the curve is planar, i.e. $\tau = 0$. The unit length used in the figures is centimetre.

We start by presenting results obtained for the equilibrium problem. We find the solutions with $\partial C/\partial t = 0$ and $\partial\phi/\partial t = 0$. These are the equilibrium states for auxin transport and grain pattern orientation.

### 3.1. Straight cylinder

In this case, cambial surface is described by a cylinder parameterized with $\vec{p}(s) = s\vec{z}$. It is easy to verify that $C = J_0/v$, $\phi = -\pi/2$ is solution of the PDE system. Auxin distribution is homogeneous along the cambium and cambial cells point in the direction of gravity. For a cylinder of radius of 10 cm and height of 100 cm, the relative errors between numerical and theoretical solutions are less than $10^{-4}$ for $C$ and $\phi$. More precisely, if $\phi_{num}$ and $C_{num}$ are the numeric solutions, $|(\phi_{num}+(\pi/2))/(\pi/2)|\leqslant 6\times10^{-5}$ and $|(C_{num}-(J_0/v))/(J_0/v)|\leqslant 2\times10^{-4}$.

We now study perturbations of the precedent problem with trees presenting deformations. Geometries are constructed using cylinders and torii. For our geometries, if the gravity effect is not included (i.e. $\alpha = 0$): $C = J_0/v$, $\phi = -\pi/2$ is solution of the problem.

### 3.2. Slightly deformed tree

In this section, the deformations from the straight cylinder are quite low. Figs. 2 and 3 show two examples of results of auxin concentration distribution. Values are normalized by the mean concentration of auxin, i.e. $J_0/v$. Simulations (Fig. 2) permit to observe zones of accumulation of auxin on the lower side of the tree with respect of gravity and depletion zones on the upper side. Fig. 3 presents two distinct zones of accumulation (and two of depletion) as a consequence of the double deformation of the tree.

Fig. 4 shows an example of result for the value of orientation angle $\phi$ corresponding to the case of Fig. 2. Cambial cells are predicted to orient specifically in the zone where curvature changes. In the first deformed zone, defined by the upper torus, cells orientations are digressing from the direction ($\phi = -\pi/2$) done by the pith. This means that directions of auxin flowing lines digress at the gravity upper side, which produces a depletion zone. Conversely, they converge in the gravity lower zone, producing accumulation. Phenomenon is reverted in the lower torus that enables auxin to redistribute and recover a homogeneous pattern in the lower zone of the tree.

Figs. 5–7 show results of normalized auxin distribution in the cross-section $S_I$ of the tree of Fig. 2. Surfaces present the evolution of the solution according to the variation of one parameter of the model: $\alpha$ (which measures the intensity of gravity term) in Fig. 5, $\mu$ in Fig. 6, $D_\parallel$ (with $D_\parallel/D_\perp = 5$, constant) in Fig. 7. Model is robust toward changes in all parameters values (all data not shown). As expected, for $\alpha = 0$, distribution is homogeneous and the importance of the heterogeneity in auxin distribution increases progressively with $\alpha$ (Fig. 5). Small values of $\mu$ trigger intensive heterogeneity in the solution, whereas high values tend to homogenize it (Fig. 6). The graph shown in Fig. 7 presents the different concentrations that result upon varying the diffusion coefficient $D_\parallel$. These results exhibit only slight variations even if $D_\parallel$ is taken equal to zero. We should mention that the results also depend poorly on the value of $K$ (data not shown). Studies on the dependence of solution according to geometric parameters show that heterogeneity increases with the radius of the surface $R$ and with the angle of the torus, which defines the importance of the inclination of the tree (data not shown).

### 3.3. Highly deformed tree

Model can also be used in a highly deformed tree. Because this model considers active transport, auxin can be transported even in a horizontal or ascending trunk (Figs. 8 and 9). Patterns always contain accumulation and depletion zones according to gravity.

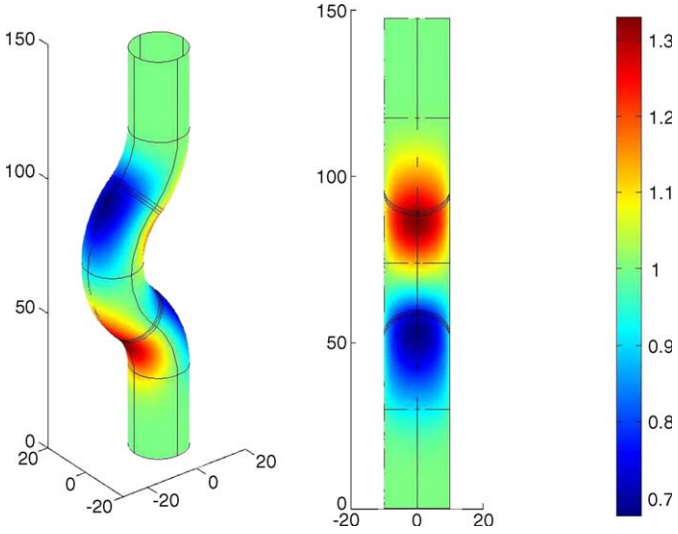


Fig. 3. Distribution of normalized auxin concentration.

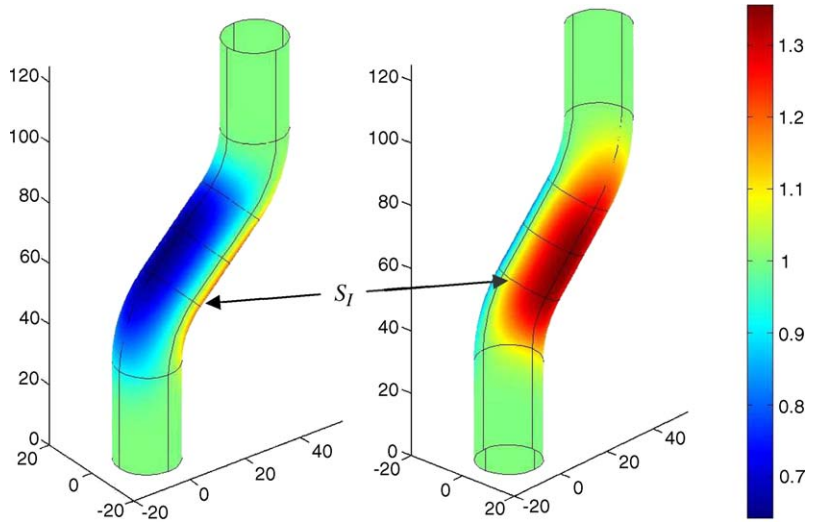


Fig. 2. Distribution of normalized auxin concentration. $S_I$ is a particular cross-section defined for this geometry, which is used in the following.

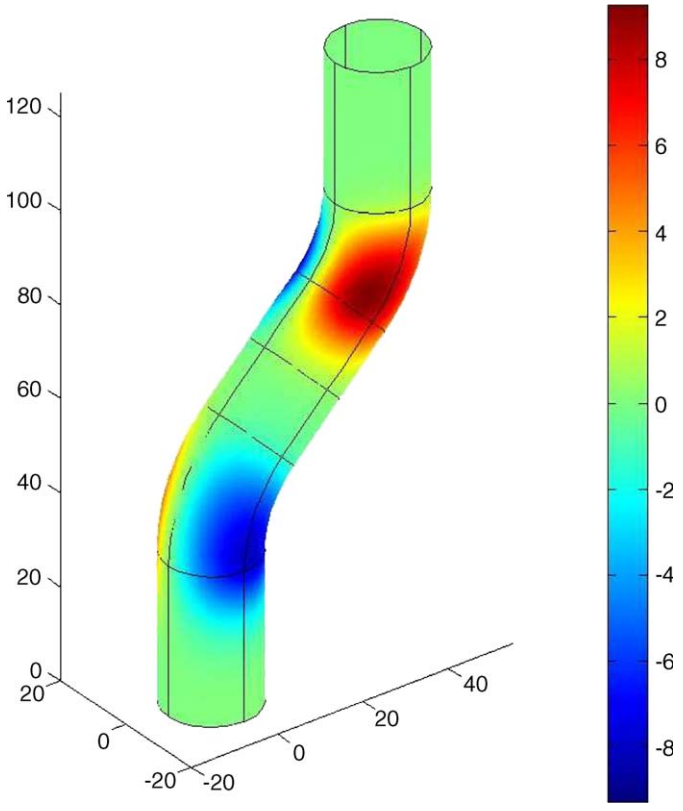


Fig. 4. Pattern of cambial cells' angle in degrees measured relative to value 90°: $((180/\pi)\phi + 90)$.

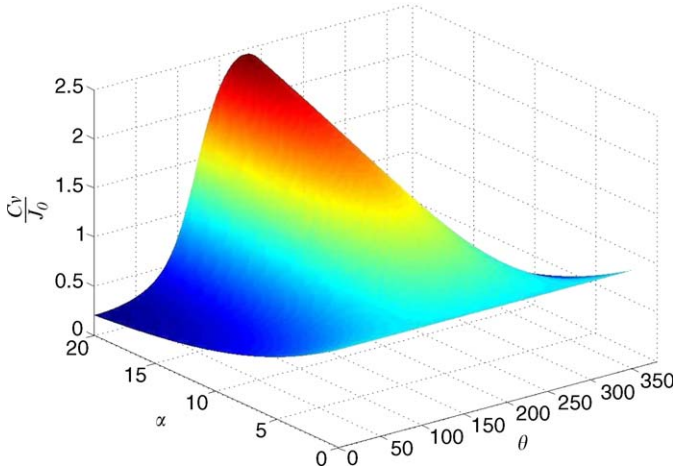


Fig. 5. Distribution of auxin in $S_I$, varying the gravity coefficient $\alpha$.

### 3.4. Time-dependent results

The model can also be run with its time-dependent term. It corresponds to the case of a straight tree deformed "instantaneously" to a curved one. At the time of the occurrence of the deformation, let suppose that the grain pattern follows the deformation. That is we use the initial condition $\phi(t_0) = -\pi/2$ and $C(t_0) = J_0/v$. The model

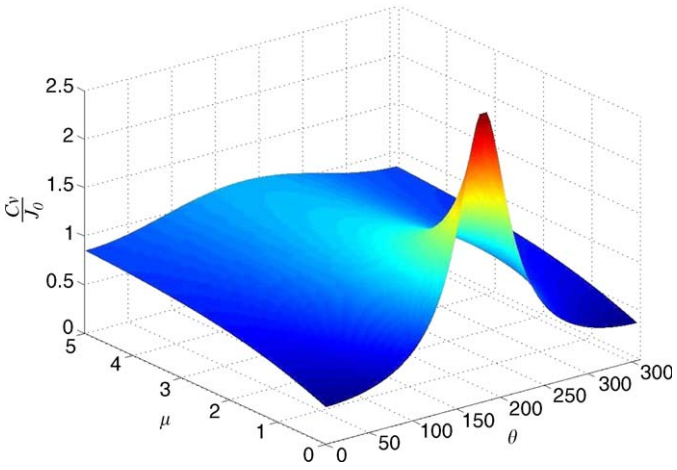


Fig. 6. Distribution of auxin in $S_I$, varying the coefficient $\mu$.

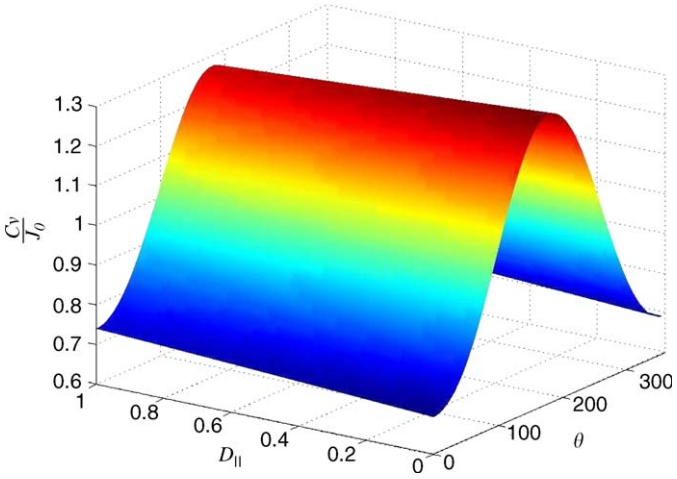


Fig. 7. Distribution of auxin in $S_I$, according to a variation of $D_{\parallel}$ from 0 to 1.

reflects the progressive formation of accumulation and depletion zones as a result of the change in auxin flowing directions (data not shown).

## 4. Radial growth

In this section, we are interested in the differential radial growth of the tree mediated by auxin. Our aim is not to quantify how much the tree grows but how growth is distributed over the trunk.

Simulating radial growth presents difficulties both from the mathematical and computational points of view. The basic idea is that the surface, which represents the trunk, mainly grows in its normal direction. The radial increment is taken as a function of the auxin concentration $C$. The simplest law, proposed by Kramer (2001), is that the radial growth is proportional to the concentration of auxin.

In our simulations, to each point $M$ in the cambial surface $S$ we associate a new point $M' = M + G(C)\vec{n}(M)$. The function $G(C)$ is the auxin-dependent law of growth

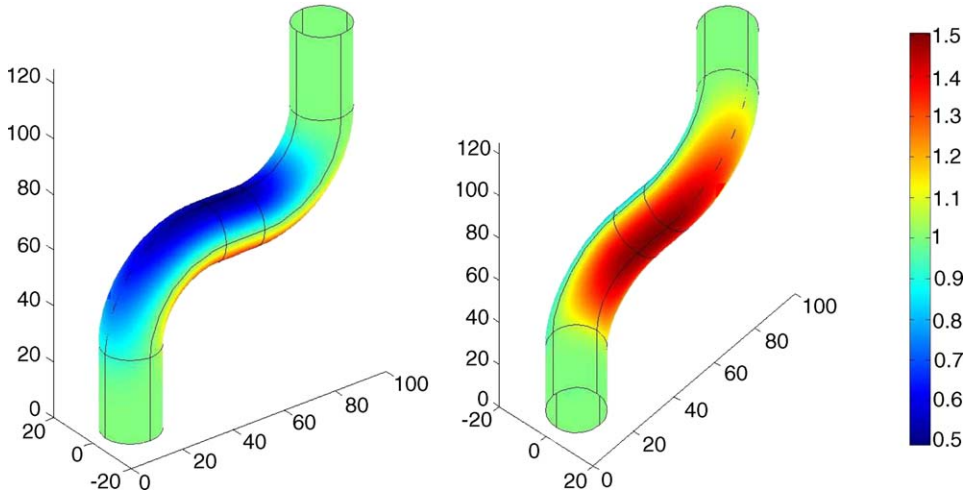


Fig. 8. Distribution of auxin in a highly deformed tree, which presents a horizontal portion.

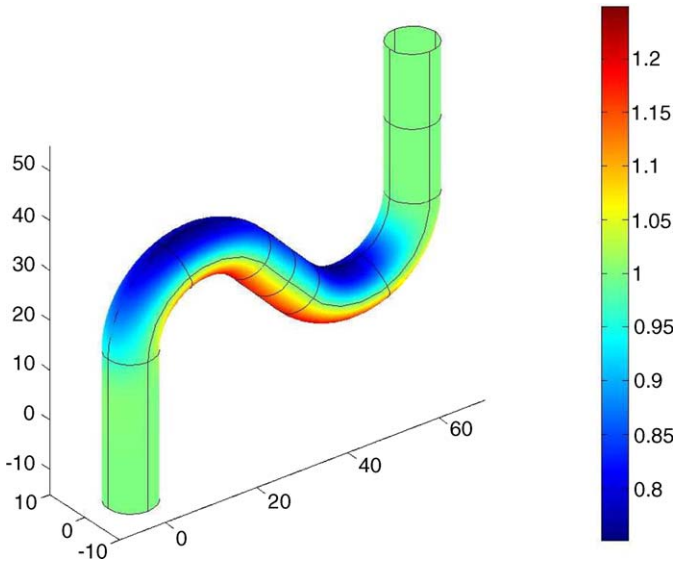


Fig. 9. Distribution of auxin in a highly deformed tree, which presents an ascending slope.

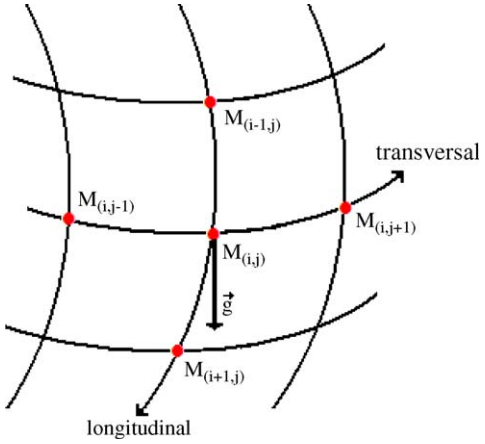


Fig. 10. Local description of discrete model elements.

and $\vec{n}(M)$ denotes the unit outer normal vector to $S$ at the point $M$. As a simple law, we set $G(C) = \alpha_1 + \alpha_2 C$. The constant $\alpha_1$ accounts for residual growth whereas $\alpha_2$ is a proportionality constant for auxin-dependent growth.

The main mathematical problem here is whether or not, the set of points $M'$ represents a new smooth surface. Indeed, if the initial surface has a highly curved portion then this law of growth would present a problem due to the crossing of the new set of points. If we consider the simple geometries given by Eq. (7), then this iteration produces a new smooth surface, if growth rates and curvature are suitably chosen.

From the computational point of view there are also important problems to be solved. Assume that the initial surface is discretized with a regular mesh (Fig. 10). Assume also that the differential problem (5) is solved using this mesh. We can apply the law of growth to each point of the mesh in order to get a new one that should represent an approximation of the iterated surface and then start the problem again. The computational problem is that this new mesh is not necessarily regular which induces errors in the solution of (5).

One way to get an approximation of this law of growth is to consider a discrete approximation of (5), replacing the curve by a polygonal line and the circles by finite regular polygons on a plane whose normal is tangent to the line. Then we use a non-homogeneous random walk on this finite set which is an approximation of a diffusion-transport equation. Each point on this mesh has four neighbours and the transition probabilities between them depend on two factors: the direction of the movement (transversal or longitudinal) and the projection of the gravity in these two directions.

Denoting $p(k, l|i, j)$ the transition probability from $M_{ij}$ to $M_{kl}$ (which are two points of the mesh), we set:

$$p(i,j+1|i,j) = a_0(1+F_{ij}), \quad p(i,j-1|i,j) = a_0(1-F_{ij}),$$
$$p(i-1,j|i,j) = b_0(1-H_{ij}), \quad p(i+1,j|i,j) = b_0(1+H_{ij})$$

with $b_0 > a_0$, $2a_0 + 2b_0 = 1$. $F_{ij}$ depends on the projection of the gravity in the transversal direction. $H_{ij}$ depends on two

factors: the projection of the gravity on longitudinal direction and another term that privileges the transport in the downward longitudinal direction.

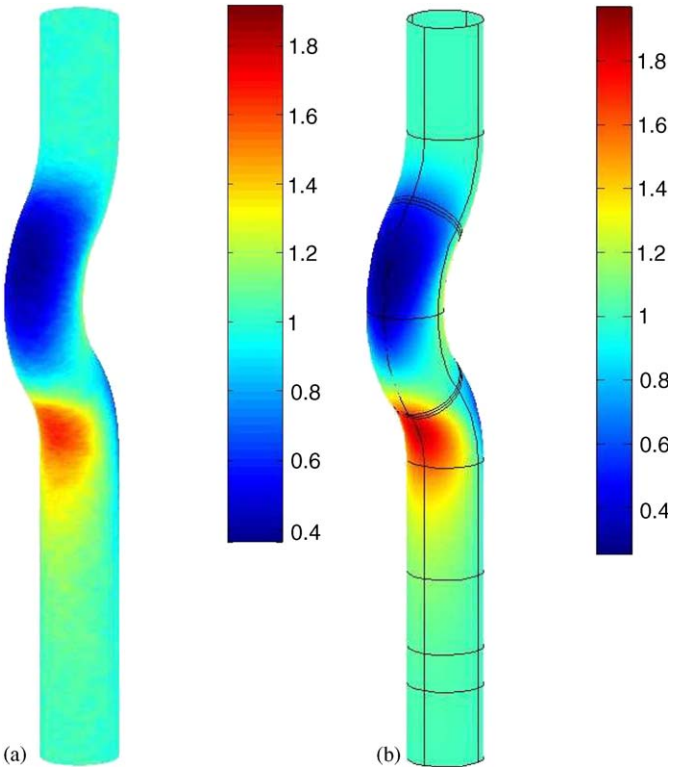


Fig. 11. Comparisons between discrete and continuous models: (a) the solution of auxin distribution obtained with the random walk model and (b) the solution from the continuous model.

In this simplified discrete approach, the dynamics of cambial cells orientation is not considered. However, lateral reallocation of auxin flux triggering accumulation is included because the principal direction of transport is longitudinal with a drift in the direction of gravity.

This model produces patterns of concentration similar to the ones of the continuous model (5). Fig. 11 shows a graphical comparison between them.

Using the law of radial growth each polygon is transformed into a new one in the same plane. This new polygon is approximated by a circle and the circle centres define a new polygonal line to start again. This method permits to iterate several steps of growth.

Fig. 12a shows a Radiata pine tree, which presents a deformation at a height of 2 m due to damage caused by European Pine Shoot Moth (*Rhyacionia buoliana*). Fig 12b is a computational reconstruction of the marked zone shown in Fig. 12a, using the methodology developed by Cominetti et al. (2002). From this reconstruction, yearly annual volume increments are calculated. Fig. 12c is the simulation obtained by our approach. The initial condition for the simulation is the geometry of the tree at the first year, approximated by a conical tubular surface. The pattern of growth is determined according to our model and the annual volume increments are adjusted to fit the real ones. Thus the values of $\alpha_1$ and $\alpha_2$ are determined for each iteration in terms of the yearly volume increment.

The external appearance of the tree does not reveal the magnitude of the initial deformation. Indeed, the tree reshapes progressively by means of differential radial growth. The model is able to reflect the evolution of the underlying pattern of differential radial growth.

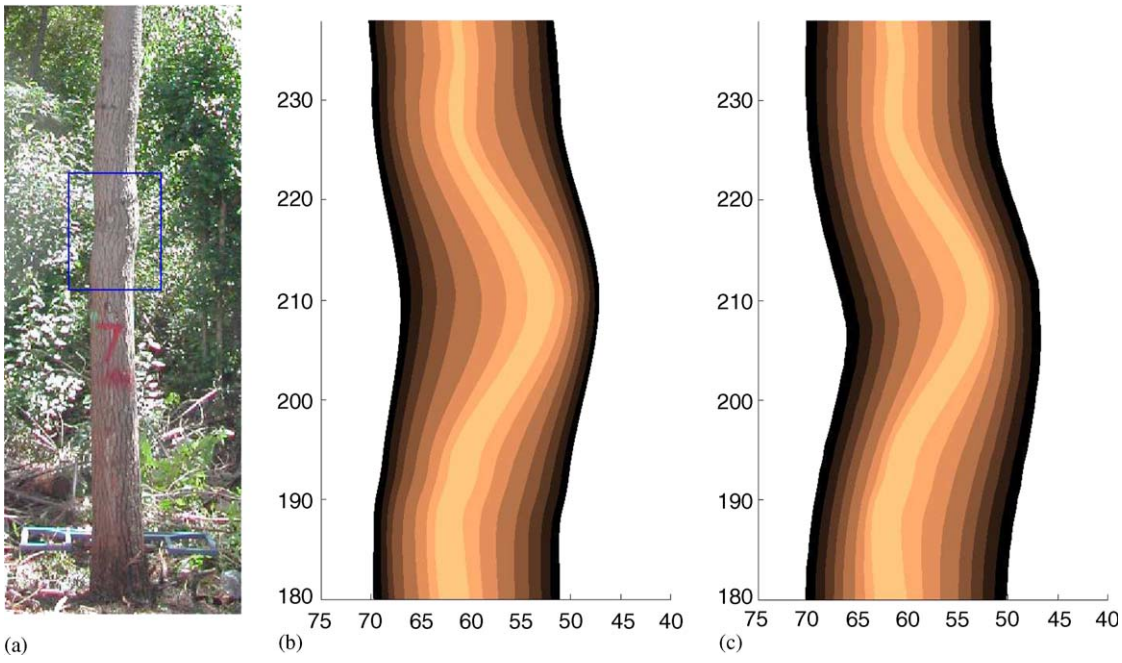


Fig. 12. (a) Photograph of a tree which presents a deformed portion (blue frame). (b) Represents the computational reconstruction made from a longitudinal section of the marked zone shown in (a). The reconstruction shows the annual growth rings for 8 years and (c) the result of the simulation over this tree for every year of growth.

## 5. Discussion and conclusions

In the first part, a model is developed for auxin transport. This new framework permits to obtain auxin concentration in a smooth surface, taking into account the influence of gravity in the transport process. In the last part, a law of growth based on auxin concentration is proposed to simulate differential radial growth over a tree.

The evolutions of patterns according to parameters variations are always coherent. For example, heterogeneity of auxin distribution increases with the weight of gravity term and diffusion terms are shown to be of minor importance with respect to active transport. We also show that the equation accounting for grain pattern dynamic used in Kramer (2002) can be extended to reflect the 3-D redistribution of auxin flux following the stimulus of gravity. However, these results need more precise experimental data in order to investigate if variables $K$, $\mu$ and function $f$ can be estimated.

The proposed law of growth only depends on IAA concentration because the aim of this paper was to explain differential growth and not growth in general. Our paper supports the idea that IAA mediates the differential growth in a conifer tree. The model can predict the allocation of the growth over the tree but does not calculate the volumetric rate of growth of the whole tree per unit of time. Obtaining a law for calculating volumetric growth requires considering many variables, which is out of the scope of this paper.

An improvement should also include mechanical considerations to deal with physical constraints of non-interpenetration during theoretical growth. The mechanical properties of tree can differ: it is well known that compression wood is denser that normal wood. This variation in mechanical properties can have an importance in the distribution of differential growth because compression wood is usually located in highly curved zones of trees. In such zones, the competition between cells for spreading is particularly intense, as they tend to grow in the same space (normal directions are converging). Thus, higher rates of cellular elimination from the cambium and some redirections of the growth normal direction appear (Forest et al., 2004; Forest and Demongeot, in press). A more realistic law of growth should be entirely 3-D as the normal growth direction can be largely disturbed: in concavities for example, some digressive component is clearly needed.

Another point to consider would be the inclusion of a regulation system of auxin metabolism, which may consider synergy with other plant hormones.

## Acknowledgement

We thank the support provided by FONDEF D011021 and Nucleus Millennium, Information and Randomness, and especially the support provided by the Centre for Mathematical Modelling (University of Chile) where the work was finally concluded.

## Appendix

In this section, we will explain the deduction of mass conservation Eq. (3). We assume for simplicity that the cambial surface $S$ is parameterized by a smooth function $r:[-L,l]\times[0,2\pi]\to\mathbb{R}^3$, where $L\gg l>0$, and $r(s,0)=r(s,2\pi)$ for all $s\in[-L,\,l]$. The tangent plane of $S$ at $r(s,\theta)$ is generated by the vectors $\partial r/\partial s$ and $\partial r/\partial\theta$. We suppose that for $s$ close to $l$ and $s\leqslant 0$, the surface $S$ is a straight cylinder, with radius $R_1$ and $R_2$, respectively, and axis parallel to $\vec{z}=(0,0,1)$, where $-\vec{z}$ gives the direction of the gravity. We are interested in the profile of auxin distribution in the portion of the *cambial surface* given by $0<s<l$, thus the condition $l\ll L$ represents the fact that dimensions of the tree are much larger than the portion considered. It is well known that for $\varepsilon>0$ sufficiently small we can define a volume $V_\varepsilon$ in $\mathbb{R}^3$, representing a cambial region, parameterized by $\Psi:[-L,l]\times[0,2\pi]\times[-\varepsilon,\varepsilon]\to\mathbb{R}^3$.

$$\Psi(s,\theta,r)=r(s,\theta)+r\frac{N(s,\theta)}{||N(s,\theta)||},\quad N(s,\theta)=\frac{\partial r}{\partial s}\wedge\frac{\partial r}{\partial\theta}.$$

It is easy to check that we can define smooth vector fields $t_{1\varepsilon}$, $t_{2\varepsilon}$, $n_\varepsilon$ such that $\|t_{1\varepsilon}\|=\|t_{2\varepsilon}\|=\|n_\varepsilon\|=1$, $t_{1\varepsilon}\perp t_{2\varepsilon}$, $t_{i\varepsilon}\perp n_\varepsilon$ for $i=1,2$ with $t_{1\varepsilon}(\cdot,\cdot,r)$, $t_{2\varepsilon}(\cdot,\cdot,r)$ tangent to the surface $S_r$ parameterized by $\Psi(\cdot,\cdot,r)$, and the vector $n_\varepsilon(\cdot,\cdot,r)$ orthogonal to $S_r$. Let $C_\varepsilon:V_\varepsilon\to\mathbb{R}$ and $\vec{J}_\varepsilon:V_\varepsilon\to\mathbb{R}^3$ denote the auxin concentration and flux, respectively. The change in auxin concentration is given by the following mass conservation equation:

$$\frac{\partial C_\varepsilon}{\partial t}=-\nabla\cdot\vec{J}_\varepsilon \text{ in } V_\varepsilon,\ t>0. \tag{8}$$

Set $\vec{u}_\varepsilon$, $\vec{w}_\varepsilon$ unitary vector fields defined in $V_\varepsilon$, with $\vec{u}_\varepsilon\perp\vec{w}_\varepsilon$ and linear combination of $t_{1\varepsilon}$, $t_{2\varepsilon}$. The vector $\vec{u}_\varepsilon$ represents the direction of active transport of auxin in the cambial region and satisfies $\vec{u}_\varepsilon=-\vec{z}$ at $s$ close to $l$ and $s\leqslant 0$. Following Fick's law, we suppose that the auxin flux $\vec{J}_\varepsilon$ can be written as

$$\begin{aligned}\vec{J}_\varepsilon=&(vC_\varepsilon-D_{||}(\nabla C_\varepsilon\cdot\vec{u}_\varepsilon))\vec{u}_\varepsilon\\&-D_\perp(\nabla C_\varepsilon\cdot\vec{w}_\varepsilon)\vec{w}_\varepsilon-D_*(\nabla C_\varepsilon\cdot\vec{n}_\varepsilon)\vec{n}_\varepsilon,\end{aligned} \tag{9}$$

where $v>0$ denotes the transport velocity, $D_{||}$ and $D_\perp$ are the longitudinal and transversal diffusion coefficients, respectively, and $D_*$ is a diffusion coefficient in the normal direction.

These coefficients satisfy $0<D_*\ll D_\perp<D_{||}$. We suppose that the flux satisfies the following boundary conditions:

$$\vec{J}_\varepsilon=-J_0\vec{z} \text{ when } s=l,-L,\ \ \theta\in[0,2\pi],\ \ r\in[-\varepsilon,\varepsilon],$$

$$\vec{J}_\varepsilon\cdot\vec{n}_\varepsilon=0 \text{ when } r=\pm\varepsilon,\ \ \theta\in[0,2\pi],\ \ s\in[-L,l].$$

Integrating Eq. (8) in a small volume described by $\{\Psi(s,\theta,r)/r \in [-\varepsilon,\varepsilon], s \in [l_1,l_2], \theta \in [\theta_1,\theta_2]\}$.

$$\frac{2}{\varepsilon}\int_{-\varepsilon}^{\varepsilon}\int_{l_1}^{l_2}\int_{\theta_1}^{\theta_2}\frac{\partial}{\partial t}C_\varepsilon(\Psi(s,\theta,r),t)\,\mathrm{d}\sigma = -\frac{2}{\varepsilon}\int_{-\varepsilon}^{\varepsilon}\int_{l_1}^{l_2}\int_{\theta_1}^{\theta_2}\nabla\vec{J}_\varepsilon(\Psi(s,\theta,r),t)\,\mathrm{d}\sigma, \quad (10)$$

where

$$\mathrm{d}\sigma = |\det\ D\Psi(s,\theta,r)|\mathrm{d}\theta\,\mathrm{d}s \sim \left|\frac{\partial r}{\partial\theta}\wedge\frac{\partial r}{\partial s}(s,\theta)\right|\mathrm{d}\theta\,\mathrm{d}s.$$

Suppose that $\nabla C_\varepsilon\cdot\vec{n}_\varepsilon \to 0$ as $\varepsilon\to 0$, and that there exists a smooth function $C$ defined in $S$, such that when $\varepsilon\to 0$ the functions $C_\varepsilon$, $\partial C_\varepsilon/\partial t$, $\nabla C_\varepsilon\cdot\vec{u}_\varepsilon$, $\nabla C_\varepsilon\cdot\vec{w}_\varepsilon$ at $(\Psi(s,\theta,r),t)$ converge to $C$, $\partial C/\partial t$, $\nabla C\cdot\vec{u}$, $\nabla C\cdot\vec{w}$ at $(\varphi(s,\theta),t)$, respectively, for $\vec{u}=\vec{u}_\varepsilon(\varphi(s,\theta),t)$, $\vec{w}=\vec{w}_\varepsilon(\varphi(s,\theta),t)$. Integrating by parts we obtain that

$$\frac{2}{\varepsilon}\int_{-\varepsilon}^{\varepsilon}\int_{l_1}^{l_2}\int_{\theta_1}^{\theta_2}\nabla\cdot[(\nabla C_\varepsilon\cdot n_\varepsilon)n_\varepsilon]\mathrm{d}\sigma\,\mathrm{d}r \underset{\varepsilon\to 0}{\longrightarrow} 0,$$

hence taking the limit as $\varepsilon\to 0$ in (10) we get that for arbitrary $\theta_1$, $\theta_2$ and $l_1$, $l_2$

$$\int_{l_1}^{l_2}\int_{\theta_1}^{\theta_2}\frac{\partial}{\partial t}C(\varphi(s,\theta),t)\,\mathrm{d}\sigma = -\int_{l_1}^{l_2}\int_{\theta_1}^{\theta_2}\nabla\cdot\vec{J}(\varphi(s,\theta),t)\,\mathrm{d}\sigma,$$

where $\vec{J}=(vC-D_{\|}(\nabla C\cdot\vec{u}))\vec{u}-D_{\perp}(\nabla C\cdot\vec{w})\vec{w}$. Therefore we have that

$$\frac{\partial C}{\partial t} = -\nabla\cdot\vec{J}\ \text{in}\ S,\ t>0,$$

$$\vec{J} = -J_0\vec{z}\ \text{when}\ s=l,-L,$$

where the gradient $\nabla$ and the divergence $\nabla\cdot$ are taken in Cartesian coordinates.

## References


Aloni, R., 2004. The induction of vascular tissues by auxin. In: Davies, P.J. (Ed.), Plant Hormones: Biosynthesis, Signal Transduction, Action!, third ed. Kluwer Academic Publishers, The Netherlands, pp. 471–492.

Bennett, M.J., Marchant, A., Green, H.G., May, S.T., Ward, S.P., Millner, P.A., Walker, A.R., Schulz, B., Feldmann, K.A., 1996. Arabidopsis AUX1 gene: a permease-like regulator of root gravitropism. Science 273, 948–950.

Chen, R., Rosen, E., Masson, P.H., 1999. Gravistropism in higher plants. Plant Physiol. 120 (2), 343–350.

Clare, E.C., Nicholas, P.H., Ottoline, L., 2000. Hormonal interactions in the control of Arabidopsis hypocotyl elongation. Plant Physiol. 124 (2), 553–561.

Cominetti, R., Padilla, F., San Martín, J., 2002. Field methodology for reconstruction a *Pinus radiata* log. N. Z. J. For. Sci. 32 (3), 309–321.

Davies, P.J., 1995. The plant hormones: their nature, occurrence and functions. In: Davies, P.J. (Ed.), Plant Hormones: Physiology, Biochemistry, and Molecular Biology. Kluwer Academic Publishers, Dordrecht, The Netherlands, pp. 1–5.

Do Carmo, M.P., 1976. Differential Geometry of Curves and Surfaces. Prentice-Hall, Inc., Englewood Cliffs, NJ 803pp.

Dolk, H.E., 1936. Growth and the geotropic substance. Rec. Trav. Bot. Neerl. 33, 509–585.

Du, S., Uno, H., Yamamoto, F., 2004. Roles of auxin and gibberellin in gravity-induced tension wood formation in *Aesculus turbinata* seedlings. IAWA J. 25 (3), 337–347.

Eklund, L., Little, C.H.A., 1998. Ethylene evolution, radial growth and carbohydrate concentrations in *Abies balsamea* shoots ringed with Ethrel. Tree Physiol. 18, 383–391.

Eklund, L., Tiltu, A., 1999. Cambial activity in 'normal' spruce *Picea abies* Karst (L.) and snack spruce *Picea abies* (L.) Karst f. *virgata* (Jacq.) Rehd in response to ethylene. J. Exp. Bot. 50 (338), 1489–1493.

Evans, M., 1991. Gravitropism: interaction of sensitivity modulation and effector redistribution. Plant Physiol. 95, 1–5.

Forest, L., Demongeot, J., in press. Cellular modelling of secondary radial growth in conifer trees: application to *Pinus radiata* (D. Don). Bull. Math. Biol.

Forest, L., San Martin, J., Padilla, F., Chassat, F., Giroud, F., Demongeot, J., 2004. Morphogenetic processes: application to cambial growth dynamics. Acta Biotheor. 52 (4), 415–438.

Friml, J., Wisniewska, J., Benkova, E., Mendgen, K., Palme, K., 2002. Lateral relocation of auxin efflux regulator PIN3 mediates tropism in Arabidopsis. Nature 415, 806–809.

Funada, R., Mizukami, E., Kubo, T., Fushitani, M., Sigiyama, T., 1990. Distribution of indole-3-acetic acid and compression wood formation in stems of inclined *Cryptomeria japonica*. Holzforschung 44, 331–334.

Gillespie, B., Thimann, K.V., 1963. Transport and distribution of auxin during tropistic response. I. The lateral migration of auxin in geotropism. Plant Physiol. 38 (2), 214–225.

Goldsmith, M.H.M., 1977. The polar transport of auxin. Annu. Rev. Plant Physiol. 28, 439–478.

Goldsmith, M.H.M., 1993. Cellular signalling: new insights into the action of the plant growth hormone auxin. Proc. Natl Acad. Sci. USA 90 (24), 11442–11445.

Goldsmith, M.H.M., Wilkins, M.B., 1964. Movements of auxin in coleoptiles of *Zea mays* L. during geotropic stimulation. Plant Physiol. 39, 151–162.

Goldsmith, M.H.M., Goldsmith, T.H., Martin, M.H., 1981. Mathematical analysis of the chemosmotic polar diffusion of auxin through plant tissues. Proc. Natl Acad. Sci. USA 78 (2), 976–980.

Han, K-H., 2001. Molecular biology of secondary growth. J. Plant Biotechnol. 3 (2), 45–57.

Harris, J.M., 1991. Formation of wood and bark. In: Kininmonth, J., Whiteside, I. (Eds.), Properties and Uses of New Zealand Radiata Pine, vol. 1. Wood properties. New Zealand Ministry of Forestry, Forest Research Institute, Wellington (Chapter 3).

Hellgren, J.M., 2003. Ethylene and auxin in the control of wood formation. Doctoral thesis, Department of Forest, Genetics and Plant Physiology, Swedish University of Agricultural Sciences.

Hellgren, J.M., Olofsson, K., Sundberg, B., 2004. Patterns of auxin distribution during gravitational induction of reaction wood in poplar and pine. Plant Physiol. 135 (1), 212–220.

Kaldeway, H., 1984. Transport and other modes of movement of hormones (mainly auxins). In: Scott, T.K. (Ed.), Hormonal regulation of development. II. The Function of hormones from the level of the cell to the whole plant, Encyclopedia of Plant Physiology (New Series), vol. 2. Springer, Berlin, pp. 80–148.

Kalev, N., Aloni, R., 1998. Role of auxin and gibberellin in regenerative differentiation of tracheids in *Pinus pinea* seedlings. New Phytol. 138 (3), 307–313.

Katekar, G.F., Geissler, A.E., 1977. Auxin transport inhibitors III. Chemical requirements of a class of auxin transport inhibitors. Plant Physiol. 60, 826–829.

Kramer, E.M., 2001. A mathematical model of auxin-mediated radial growth in trees. J. Theor. Biol. 208 (4), 387–397.

Kramer, E.M., 2002. A mathematical model of pattern formation in the vascular cambium of trees. J. Theor. Biol. 216 (2), 147–158.

Larson, P.R., 1994. The Vascular Cambium, Development and Structure. Springer Series in Wood Science. Springer, Berlin 725pp.

Little, C.H.A., Savidge, R.A., 1987. The role of plant growth regulators in forest tree cambial growth. Plant Growth Regul. 6, 137–169.

Lomax, T.L., Muday, G.K., Rubery, P., 1995. Auxin transport. In: Davies, P.J. (Ed.), Plant Hormones: Physiology, Biochemistry, and Molecular Biology. Kluwer Academic Publishers, Dordrecht, The Netherlands, pp. 509–530.

Mitchison, G.J., 1980. The dynamics of auxin transport. Proc. R. Soc. London B 209, 489–511.

Muday, G.K., Hu, S., Brady, S.R., 2000. The cytoskeleton may control the polar distribution of an auxin transport protein. Gravitational Space Biol. Bull. 13 (2), 75–83.

Ottenschläger, I., Wolff, P., Wolverton, C., Bhalerao, R., Sandberg, G., Ishikawa, H., Evans, M., Palme, K., 2003. Gravity-regulated differential auxin transport from columella to lateral roots cap cells. Proc. Natl Acad. Sci. USA 100 (5), 2987–2991.

Parker, K., Briggs, W., 1990. Transport of indole-3-acetic acid during gravitropism in intact maize coleoptiles. Plant Physiol. 94 (4), 1763–1769.

Phelps, J.E., McGuiness, E.A., Smolinski, M., Saniewski, M., Pieniasek, J., 1977. A note on the formation of compression wood induced by morphactin IT3456 in *Thuja* shoots. Wood Fiber Sci. 8 (4), 223–227.

Plomion, C., Pionneau, C., Brach, J., Costa, P., Bailleres, H., 2000. Compression wood-responsive proteins in developing xylem of Maritime pine (*Pinus pinaster* Ait.). Plant Physiol. 123 (3), 959–969.

Rashotte, A.M., Brady, S.R., Reed, R.C., Ante, S.J., Muday, G.K., 2000. Basipetal auxin transport is required for gravitropism in roots of Arabidopsis. Plant Physiol. 122 (2), 481–490.

Rashotte, A., Poupart, J., Waddell, C.S., Muday, G., 2003. Transport of the two natural auxins, indole-3-butyric acid and indole-3-acetic acid, in Arabidopsis. Plant Physiol. 133 (2), 761–772.

Rubery, P.H., Sheldrake, A.R., 1974. Carrier-mediated auxin transport. Planta 118, 101–121.

Sundberg, B., Little, C.H.A., Cui, K., Sandberg, G., 1991. Level of endogenous indole-3-acetic acid in the stem of *Pinus sylvestris* in relation to seasonal variation of cambial activity. Plant Cell Environ. 14, 241–246.

Sundberg, B., Tuominen, H., Little, C.H.A., 1994. Effects of the indole-3-acetic acid (IAA) transport inhibitors N-1-naphtylphthalamic acid and morphactin on endogenous IAA dynamics in relation to compression wood formation in 1-year old *Pinus sylvestris* L. shoots. Plant Physiol. 10 (2), 469–476.

Uggla, C., Moritz, T., Sandberg, G., Sundberg, B., 1996. Auxin as positional signal in pattern formation in plants. Proc. Natl Acad. Sci. USA 93, 9282–9386.

Uggla, C., Mellerowicz, E.J., Sundberg, B., 1998. Indole-3-acetic acid controls cambial growth in scots pine by positional signaling. Plant Physiol. 117 (1), 113–121.

Wang, Q., Little, C.H.A., Odén, P.C., 1997. Control of longitudinal and cambial growth by gibberellins and indole-3-acetic acid in current-year shoots of *Pinus sylvestris*. Tree Physiol. 17, 715–721.

Wardrop, A.B., Davies, G.W., 1964. The nature of reaction wood. VIII. The structure and differentiation of compression wood. Aust. J. Bot. 12 (1), 24–38.

Yamaguchi, K., Itoh, T., Shimaji, K., 1980. Compression wood induced by 1-*N*-naphtylphthalamic acid (NPA), an IAA transport inhibitor. Wood Sci. Technol. 14, 181–185.